X-ray Scattering Study of Early Stage Spinodal Decomposition in Al$_{0.62}$Zn$_{0.38}$

J. Mainville,* Y. S. Yang,[†] K. R. Elder,[‡] and M. Sutton

Centre for the Physics of Materials and Department of Physics, McGill University, Montreal, Canada H3A 2T8

K. F. Ludwig, Jr.* and G. B. Stephenson[§]

IBM Research Division, Thomas J. Watson Research Center, Yorktown Heights, New York 10598
(Received 22 November 1996)

In situ small-angle x-ray scattering studies of the spinodal decomposition kinetics in an AlZn alloy at the critical composition have been performed with a time resolution of 10 ms. The kinetics of fluctuation relaxation above the critical point merges smoothly with the early-stage kinetics of fluctuation growth below T_c. Strong nonlinearities are present at the earliest times measured, even above the critical point. The nonlinear theory of Langer, Bar-on, and Miller [Phys. Rev. A **11**, 1417 (1975)] quantitatively fits the data with reasonable thermodynamic and transport parameters. [S0031-9007(97)02875-5]

The processes by which new phases are formed during a phase transformation are important in determining the microstructure of many materials. Spinodal decomposition is one of the simplest mechanisms for the initiation of such processes since the composition fluctuations present in the single-phase state grow continuously to form the regions of the segregated phases. Most theories of phase transition kinetics are based on an extension of equilibrium thermodynamics to provide the "driving force" for the transition. A quantitative comparison of the thermodynamic and kinetic parameters obtained from measurements of spinodal decomposition kinetics to those derived from conventional phase equilibria and transport measurements is a way to test these concepts. Such a test should involve measurements of kinetics both above and below the critical temperature T_c, since the equilibration of fluctuations above T_c occurs by the same physical processes as the early stages of phase separation below T_c. Studies at the critical composition reduce the occurrence of phase separation initiated by nucleation above the spinodal region.

Metal alloys are an important class of materials which also provide excellent model systems to quantitatively test theories of spinodal decomposition. An ideal probe of the time evolution in these systems is small-angle x-ray scattering. The classic metal alloy for studies of spinodal decomposition is AlZn. It has a fairly symmetric equilibrium miscibility gap bounded by simple face-centered-cubic substitutional alloy phases with similar lattice constants, its equilibrium properties are well characterized, and it has good x-ray contrast. The gap terminates at a Zn atom fraction $c = 0.395$ and $T = 624.5$ K [1]. The difference in lattice constants between the two phases introduces strains and the coherent critical point [2] is located at $c = 0.38$ and $T_c = 597$ K [3]. It is this critical point that is relevent to early time studies. Many studies of kinetics [4,5] have been performed on the AlZn system, but none near or above the critical point. This is because

the time scale for the transition becomes quite short (<1 s) at these temperatures. In this Letter, we present measurements on the early time spinodal decomposition in AlZn at the critical composition, both near and above the critical point with millisecond time resolution.

All spinodal systems are expected to cross over to a nonlinear scaling regime at late times. For early times, systems with long-range forces are expected to exhibit linear mean field behavior, while for systems with short-range forces the effects of thermal fluctuations are expected to make even the early time behavior nonlinear [6]. Most studies of spinodal decomposition have focused on the long time scaling behavior and only a few experimental studies have given detailed results for early times [7–11]. Experiments on glasses [8] and polymers [9] have shown that linear theories can work well for these long-range-force systems. On the other hand, nonlinear effects have clearly been seen in binary liquids [10] and alloys [11]. While these studies present a qualitative comparison to theory, there has yet to be a quantitative and comprehensive comparison of experiment to nonlinear early stage spinodal decomposition theory.

Although several approaches exist to handle the nonlinearity [6,12], we use our data to provide a critical test of a nonlinear computation scheme introduced by Langer, Bar-on, and Miller (LBM) [13]. This method can handle large nonlinearities; however, it is based on an uncontrolled approximation scheme [14] and breaks down very close to T_c. An experimental test with measurements near T_c should provide further insight.

The experiments were performed on the IBM-MIT beam line X20C at the National Synchrotron Light Source. This beam line has been optimized for time-resolved scattering measurements with the use of a wide-bandpass ($\Delta\lambda/\lambda \sim 1\%$) multilayer monochromator which yields a flux of $\sim 10^{13}$ photons/s at $\lambda = 2.07$ Å. The scattering was collected in transmission by a linear position-sensitive

detector at wave vectors q in the range 0.008 to 0.085 Å^{-1}, with a resolution which varied from 0.0024 to 0.0017 Å^{-1} across the range. A detailed description of the experimental setup has been published [15].

The samples studied were melt-spun polycrystalline $Al_{0.62}Zn_{0.38}$ ribbons $\sim 18\,\mu m$ thick with a grain size of $\sim 1\,\mu m$. During a typical temperature cycle, a ribbon was resistively self-heated in a He atmosphere to an anneal temperature T_a in the single-phase region, well above T_c, and then quenched to a constant (± 1 K) aging temperature T_q by rapidly adjusting the heating power. Quenches of ~ 150 K could be achieved in less than 100 ms. X-ray scattering patterns and the sample temperature were simultaneously recorded every 10 ms. The time at which T_q is reached, defined as $t = 0$, can be determined to within 5 ms. The sample was subjected to repeated annealing and aging cycles in order to investigate different T_q. To test reproducibility, identical temperature cycles were sometimes repeated with no changes in the results. The temperature was monitored using an infrared pyrometer calibrated such that the measured T_c agreed with the literature value.
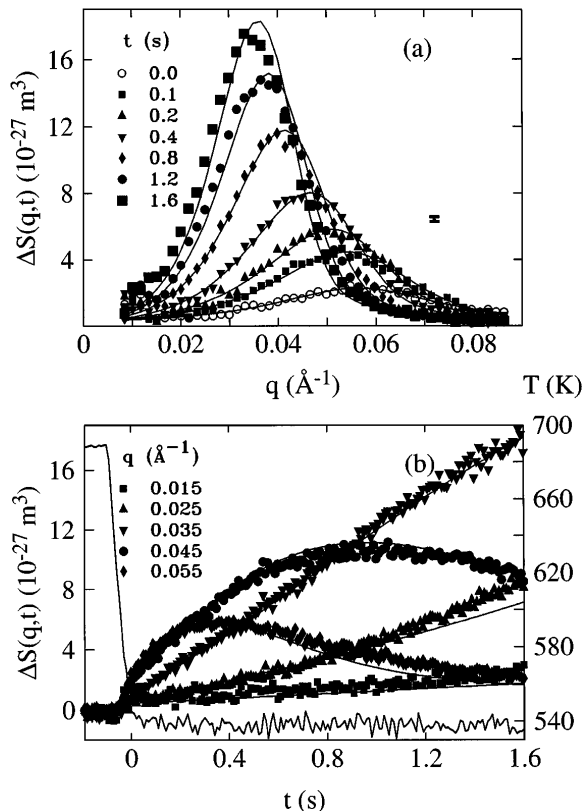
Figure 1 shows the structure factor evolution for a quench from 690 to 541 K. The solid lines are fits as discussed below. The scattering intensity has been normalized to obtain structure factors $S(q,t)$ in absolute units [8]. Figure 1(a) shows $\Delta S(q,t)$ which is defined as $S(q,t)$ minus the prequench scattering pattern. This removes any constant background scattering and the grain boundary scattering intrinsic to polycrystalline samples, but it also removes the scattering from equilibrium fluctuations at T_a. For each time $\Delta S(q,t)$ peaks as a function of q. With increasing time this peak moves towards smaller q and gets sharper. $\Delta S(q,t)$ displays the "crossing of the tails" typical of nonlinear behavior [11]. The $t = 0$ scan also has a peak which reflects the structure that develops during the quench. Figure 1(b) shows the time evolution of $\Delta S(q,t)$ at selected wave vectors. Even at the short times investigated here, $\Delta S(q,t)$ is nonmonotonic in time, clearly not following the exponential growth law predicted by linear theory [16].

Figure 2 presents the structure factor $\Delta S(q,t)$ after a quench from 690 to 599 K, showing the reequilibration of fluctuations in the single-phase region. It is clear that the time resolution of the measurement is sufficient to observe the kinetics of the fluctuations above T_c, and
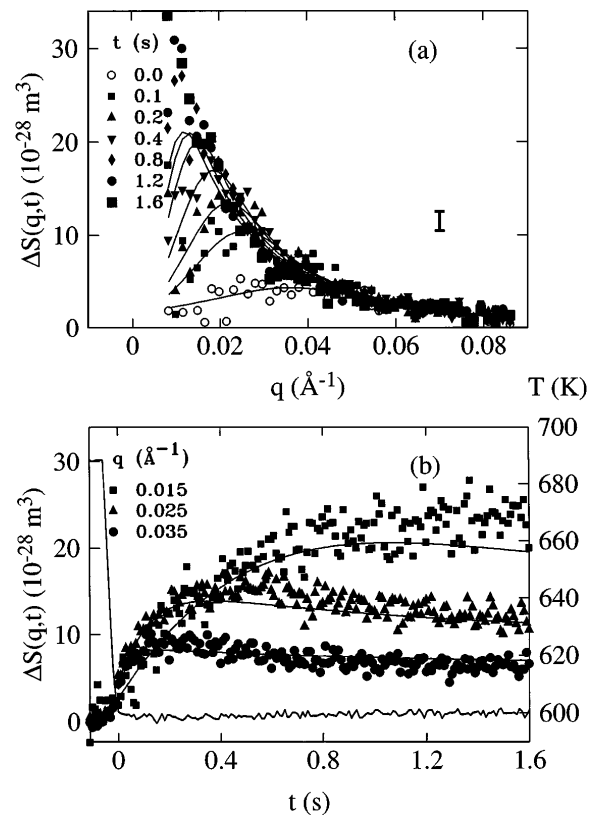
FIG. 1. (a) Evolution of the structure factor at $T_q = 541$ K (below T_c). The subtracted prequench scattering ranged from 22×10^{-27} m^3 at 0.01 Å^{-1} to 0.06×10^{-27} m^3 at 0.08 Å^{-1}. Solid lines show the best fit to LBM. The bar represents errors. (b) Constant-q slices through $\Delta S(q,t)$ and corresponding LBM theory curves. The bold line shows the temperature during the quench and during aging.

FIG. 2. (a) Evolution of the structure factor at $T_q = 599$ K (above T_c). Solid lines show the best fit to LBM. The bars represents errors. (b) Constant-q slices through $\Delta S(q,t)$ and corresponding LBM curves. The bold line shows the temperature during the quench and during aging.

thus also to observe the early stage kinetics below T_c. As for quenches into the unstable region, a nonmonotonic behavior is observed in the time evolution [Figure 2(b)], indicating nonlinear kinetics even during reequilibration in the single-phase region. By comparing a series of measurements at various temperatures, we observe that the early stage behavior below T_c smoothly crosses over to that above.

The LBM equation for $S(q,t)$ at the critical composition c_0 is given by

$$\frac{\partial S(q,t)}{\partial t} = -2Mq^2\left[\left(\kappa q^2 + \frac{\partial^2 f}{\partial c^2}\right)_{c_0} S(q,t) + \frac{1}{6}\left(\frac{\partial^4 f}{\partial c^4}\right)_{c_0} S_4(q,t)\right] + 2Mk_BTq^2.$$

Here f is the volume free energy of alloy of composition c, κ is the gradient free energy coefficient, M is the mobility, and $S(q,t)$ and $S_4(q,t)$ are the Fourier transforms of the 2nd- and 4th-order two-point correlation functions, respectively. The closing scheme proposed by LBM assumes that the q dependence of $S_4(q,t)$ is derivable from $S(q,t)$ and that the composition probability distribution can be taken as the sum of two Gaussians with associated peak positions $\pm b(t)$ and width $\sigma(t)$. The increasing separation of the two peaks governs the process of phase separation.

Given an initial structure factor $S(q,0)$ at time $t = 0$, and an initial value for either b or σ, the LBM algorithm will generate $S(q,t)$. We obtained $S(q,0)$ from the measured quenched-in structure change $\Delta S(q,0)$, parametrized by a Lorentzian, by adding back in the scattering from the equilibrium fluctuations at T_a. This contribution, which is the same for all data sets, is obtained from an analysis of the equilibrium scattering at temperatures above T_c. Although small (0.051×10^{-27} m^3 at 0.01 Å^{-1}), it is included for completeness. It is subsequently subtracted from the LBM-generated $S(q,t)$ in order to compare to the measured $\Delta S(q,t)$. In our fits the initial value of b is used as a parameter, and $\sigma(0)$ is calculated from $S(q,0)$.

To complete the model, a Landau-Ginzburg quartic coarse-grained free energy is used: $f(c) = \frac{1}{2}r(c - c_0)^2 + \frac{1}{4}u(c - c_0)^4$. An intrinsic part of f is the wave vector cutoff q_{max} which is related to a coarse graining length and is needed to truncate the diverging integrals. The least-squares fitting procedure was initially formulated in terms of the parameters κ, M, r, u, q_{max}, and $b(0)$. It was found that these parameters overdetermine the fits and that when q_{max} is assumed independent of T and r, an unphysical increase of $|r|$ as T approaches T_c is obtained. However, as proposed by LBM, when q_{max} is constrained to be proportional to the inverse correlation length, $\xi^{-1} = \sqrt{-2r/\kappa}$ (below T_c) or $\sqrt{r/\kappa}$ (above T_c), the fitting procedure converges and results in the expected decrease of $|r|$ as T_c is approached. The constant $\alpha \equiv q_{max}\xi$ could be varied within the range 0.5 to 3.0 without affecting the quality of the fits, provided r

is divided by α^2 and u by α^3. The fits thus determine a unique value of q_{max} for each T, which is larger for deeper quenches (0.375 Å^{-1} at 541 K) and is a minimum for the data closest to T_c (0.084 Å^{-1} at 597 K). Both κ and M are unaffected by the choice of α. For this analysis, $\alpha = 1$ has been used. In summary, only the five parameters κ, r, u, M, and $b(0)$ are adjusted during the fits and they suffice to fit the early time evolution for each temperature.

Least-squares fits of the LBM equation of motion to the measured $\Delta S(q,t)$ have been made for all temperatures investigated. The solid lines in Figs. 1 and 2 show the results of two such fits. All fits have comparable quality to those in Figs. 1 and 2, fits for $T < T_c$ being better than those for $T > T_c$. Clearly this model effectively parametrizes the early time data. Limiting the fits to the first 0.2 s of the complete 1.6 s of the data sets has little effect on the best-fit values of the parameters [17].

Fitting the measured $\Delta S(q,t)$ to a linear equation of motion [16,18] did not work well, even for short times. An estimate of the nonlinearity [6] is given by $\epsilon \equiv (k_BTu/r^2)(r/\kappa)^{3/2}$. Using the best-fit values at 541 K, $\epsilon = 32.45 \pm 0.09$ and each 10 ms corresponds to a reduced time $\tau \equiv 2Mr^2t/\kappa = 51.7 \pm 0.3$. These numbers indicate a highly nonlinear situation.

In Figure 3, the best fit values of the parameters for all aging temperatures are compared on an absolute scale with independent estimates obtained from conventional measurements. Estimates for r and u were obtained from analysis of the equilibrium phase diagram [3]; κ was estimated from a model [18] assuming nearest neighbor interactions. The mobility, M, is compared to the value calculated from the diffusivities [19]. Since the Al tracer diffusivity D_{Al}^* is not known, Fig. 3(d) shows the mobility obtained by using the measured Zn tracer diffusivity [20] and assuming $D_{Zn}^*/D_{Al}^* = 3$.

Well below T_c, the best-fit values from LBM agree remarkably well with the values from conventional measurements. This provides quantitative support both for the applicability of LBM in this region and, more generally, for the use of equilibrium thermodynamics to provide the driving force for the transition. The agreement for r and u shows that the use of $\alpha = 1$ is reasonable. However, above T_c the best-fit values for u are unreasonably large. Constraining $u = 4 \times 10^9$ J/m^3 results in slightly worse fits. It is not clear that the probability distribution used by LBM is appropriate in the single-phase region. As T_c is approached from below, the best-fit values of all four parameters show systematic deviations from the estimated temperature dependence. This may mean that there is an increasing discrepancy between LBM and the data, or alternatively, that LBM gives "effective" values which deviate near T_c.

In this study, *in situ* x-ray scattering, high quench rates, and millisecond time resolution have enabled a detailed study of early stage spinodal decomposition at
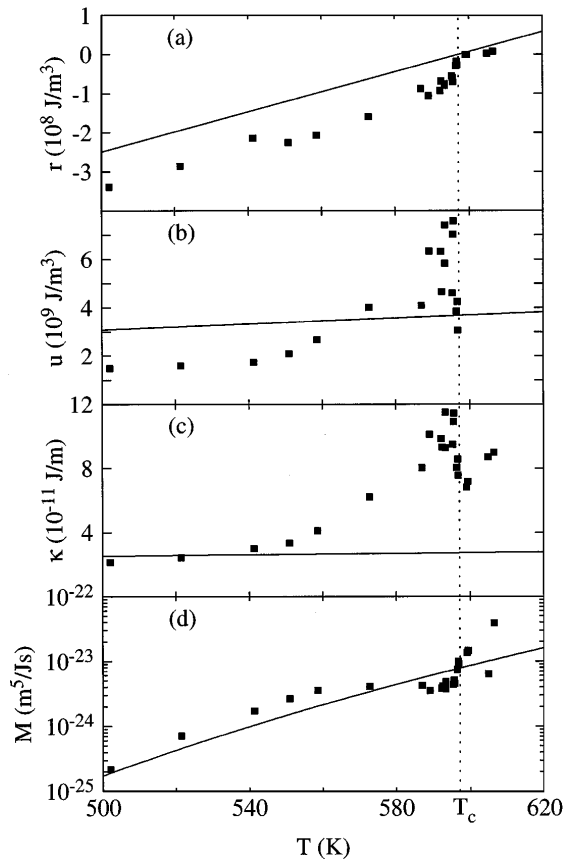
FIG. 3. Least-squares parameters from fits to LBM. The solid lines are independent estimates from phase equilibria (a)–(c) and from tracer diffusion (d). The values of u above T_c (not plotted) are 191, 379, 40, and 17×10^9 J/m^3 in order of increasing T. The parameter $b(0)$ (not plotted) increases with the depth of the quench and scales with the integrated intensity of $\Delta S(q, 0)$.

the critical composition in AlZn. This is a powerful and general technique to study phase transition kinetics which can be significantly enhanced now that third generation synchrotron sources have come on line.

   *Present address: Department of Physics, Boston University, Boston, MA 02215.

   †Present address: Department of Physics, RCDAMP, Pusan University, Pusan, Korea 609-735.

   ‡Present address: Department of Physics, Oakland University, Oakland, MI 48309-4401.

   §Present address: Materials Science Division, Argonne National Laboratory, Argonne, IL 60439.

[1] M. Hansen, *Constitution of Binary Alloys* (McGraw-Hill, New York, 1958), p. 148.

[2] J. W. Cahn, Acta Metall. **9**, 795 (1961).

[3] The coherent spinodal is calculated from a regular solution parametrization of the miscibility line [J. Lašek, Czech. J. Phys. B **15**, 848 (1965)] and measured temperature-dependent elastic constants [B. K. Kardasev, S. P. Nikanorov, and J. Lašek, Czech. J. Phys. B **18**, 275 (1968)].

[4] K. B. Rundman and J. E. Hilliard, Acta Metall. **15**, 1025 (1967).

[5] J. J. Hoyt *et al.,* Acta Metall. **37**, 1597 (1989), and references therein.

[6] M. Grant *et al.,* Phys. Rev. B **31**, 3027 (1985).

[7] B. D. Gaulin, S. Spooner, and Y. Morii, Phys. Rev. Lett. **59**, 668 (1987); M. Furusaka, Y. Ishikawa, and M. Mera, Phys. Rev. Lett. **54**, 2611 (1985); J. C. LaSalle and L. H. Schwartz, Acta Metall. **34**, 989 (1986).

[8] G. B. Stephenson *et al.,* Phys. Rev. B **43**, 13 417 (1991).

[9] F. S. Bates and P. Wiltzius, J. Chem. Phys. **91**, 3258 (1989).

[10] N. C. Wong and C. M. Knobler, J. Chem. Phys. **69**, 725 (1978); Y. C. Chou and W. I. Goldburg, Phys. Rev. A **20**, 2105 (1979).

[11] For a review, see J. D. Gunton, M. San Miguel, and P. S. Sahni, in *Phase Transitions and Critical Phenomena,* edited by C. Domb and J. L. Lebowitz (Academic Press, New York, 1983), Vol. 8.

[12] G. F. Mazenko, O. T. Valls, and M. Zannetti, Phys. Rev. B **38**, 520 (1988).

[13] J. S. Langer, M. Bar-on, and H. D. Miller, Phys. Rev. A **11**, 1417 (1975).

[14] For a test of the LBM scheme using a numerical solution of a Langevin equation, see K. R. Elder, T. M. Rogers, and R. C. Desai, Phys. Rev. B **38**, 4725 (1988).

[15] G. B. Stephenson, Nucl. Instrum. Methods Phys. Res., Sect. A **266**, 447 (1988).

[16] H. E. Cook, Acta Metall. **18**, 297 (1970).

[17] Longer runs (60 s) showed that the LBM fits deteriorate for longer times. At 541 K, the fit breaks down for $t > 2.0$ s. The scaling regime appears to start at $t \sim 10$ s.

[18] J. W. Cahn and J. E. Hilliard, J. Chem. Phys. **28**, 258 (1958).

[19] G. B. Stephenson, Scripta Metall. **20**, 465 (1986).

[20] I. Gödény *et al.,* Z. Metallkd. **72**, 97 (1981). We interpolated for $c = 0.38$ to get $D^*_{Zn} = (1.8 \times 10^{-5} \text{ m}^2/\text{s}) \exp(-1.69 \times 10^{-19} \text{ J}/k_B T)$.